COMPDYN 2015
5th ECCOMAS Thematic Conference on
Computational Methods in Structural Dynamics and Earthquake Engineering
M. Papadrakakis, V. Papadopoulos, V. Plevris (eds.)
Crete Island, Greece, 25–27 May 2015

FINITE ELEMENT ELASTIC ANALYSIS OF 3-D FLEXIBLE PAVEMENTS UNDER MOVING LOADS

Niki D. Beskou[1], Stefanos V. Tsinopoulos[2], and Dimitrios D. Theodorakopoulos[1]

[1] Department of Civil Engineering
University of Patras, GR-26504, Greece
e-mail: nikidiane@gmail.com, d.d.theod@upatras.gr

[2] Department of Mechanical Engineering
Technological Educational Institute of Western Greece, Patras, GR-26334, Greece
e-mail: stsinop@gmail.com

Keywords: Flexible Pavements, Moving Loads, Elastodynamics, Finite Elements, Uniform and Layered Half-space.

Abstract. *The dynamic response of flexible road pavements to moving vehicles is numerically obtained by the time domain finite element method under 3-dimensional conditions with the aid of the commercial program ANSYS. Both the uniform and layered elastic half-space are considered. The moving with constant speed loads (wheels) of the vehicle are simulated by assigning time dependent load values at all the surface nodes along the vehicle path, which are activated at the time it takes for every wheel to travel the distance from the origin to every node's location. Simple supports on rollers and viscous absorbing boundaries of the pavement domain are both considered. Comparisons with analytical exact solutions for the half-space model under moving loads and analytical approximate solutions for the layered half-space model under static loads are made for validation and comparison reasons, respectively. The cases of static versus dynamic loads, of single load versus a series of loads and of low versus high vehicle's velocity are also compared and discussed from the viewpoint of how they affect the response of the pavement.*

1 INTRODUCTION

During the last 25 years or so, a lot of research on the analysis and design of flexible and rigid pavements under moving vehicles and realistic geometries with the aid of numerical methods, such as the finite element method (FEM), has been successfully conducted [1,2]. The vehicle models can be either concentrated or distributed loads moving with constant speeds, or more complicated ones involving spring-mass-damping systems with variable speed. The pavement models can be simple beams or plates on Winkler elastic foundations or layered half-spaces under conditions of plane strain or full three-dimensionality [2].

Eventhough some works dealing with nonlinear pavement behavior have appeared recently, most of the works on pavement dynamics are associated with linear elastic material behavior including viscoelasticity and poroelasticity [2]. Due to the complexity of vehicle and pavement modeling even when elastic material behavior is assumed, use of numerical methods, such as the FEM, is imperative.

Flexible pavements, modeled as elastic layered half-spaces under stationary or moving loads, have been analysed by various numerical methods such as the FEM, the boundary element method (BEM) or the layered system theory in matrix form [3-8].

In this work, the FEM is employed for the numerical determination of the response of flexible pavements composed of three layers on deformable soil to constant speed moving vehicles consisting of multiple axles under three-dimensional conditions. The material behavior of the layers and the supporting soil is assumed to be linear elastic. The FEM is employed and used in the time domain with the aid of the commercial computer program ANSYS [9].

Three- dimensional solid finite elements are used for the discretization of the space domain. Nonreflecting viscous boundaries at the four vertical faces and the bottom horizontal face of the pavement domain as well as nodal springs at the bottom face are introduced in ANSYS on the basis of the theories described in [10] and [11]. The moving with constant speed loads (wheels) of the vehicle are simulated by assigning time dependent load values at all the surface nodes along the vehicle path, which are activated at the time it takes for every wheel to travel the distance from the origin to every node's location. This process is provided to ANSYS through an attached to it computer program.

The above mentioned FEM is validated by comparing it with the analytical solutions involving the elastic half-space under a single, vertical, concentrated or equivalent distributed moving or stationary load [12, 13] and the elastic layered half-space under a distributed vertical static load [14]. Further numerical studies are also made to investigate the cases of static versus dynamic loading, of a single load versus a series of loads and of low versus high velocity of vehicles in order to determine their effects on the pavement response.

2 FINITE ELEMENT MODELING OF PAVEMENT STRUCTURE

Half of a typical three layer flexible road pavement structure in a three-dimensional (3-D) space is shown in Fig.1 with the plane zx to be the plane of symmetry. This structure has dimensions 29.45 m along the vertical z direction, 15.00 m along the lateral (transverse) y direction and 30.00m along the longitudinal x direction and is supported by a deformable soil. It consists of three elastic layers fully bonded to each other and to the supporting soil with the top one being the surface asphaltic layer of thickness 0.15 m, the intermediate one, the granular base layer, of thickness 0.30 m and the bottom one, the subgrade layer, of thickness 6.00 m. The material properties of the layers are E_1 = 1000 MPa, v_1 = 0.35, ρ_1 = 2500 kg/m^3 for the top layer, E_2 = 400 MPa, v_2 = 0.35, ρ_2 = 2100 kg/m^3 for the intermediate layer and E_3 = 80 MPa, v_3 = 0.40, ρ_3 = 2000 kg/m^3 for the bottom layer, where E, v and ρ denote modulus of elasticity, Poisson's ratio and mass density, respectively.

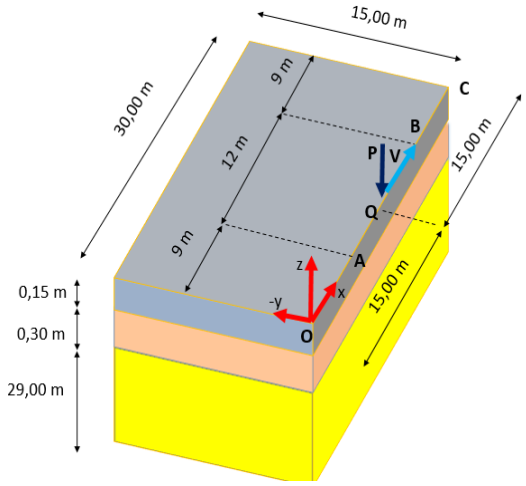

Figure 1: The three layered road pavement structure.

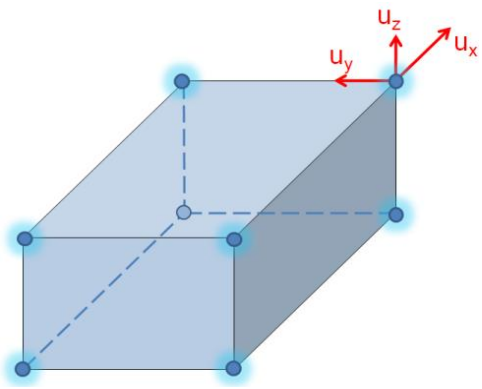

Figure 2: The 8-node 3-D finite element (SOLID185, with 24 d.o.f.)

The above pavement structure is discretized into a finite number of 8-noded 3-D solid elements (bricks) as shown in Fig.2 symbolized as SOLID185 in the commercial computer program ANSYS [9] and having in total 24 degrees of freedom (d.o.f.). The thickness of these elements increases as one goes from top to bottom of the structure. After some trials one can finally end up with an optimum discretization consisting of 145920 elements or 155961 nodes (3*155961 = 467883 d.o.f.).

Because the three vertical faces (the fourth one is the zx plane of symmetry) and the bottom horizontal face of the pavement structure are artificial boundaries, waves generated by the motion of the vehicle along the surface of the pavement propagate inside the pavement domain are reflected at those artificial boundaries and pollute the wave propagation inside the domain. For this reason, one usually introduces absorbing or non-reflecting devices at those boundaries. The most widely used absorbing boundaries because of their simplicity, are the standard viscous boundaries of Lysmer and Kuhlemeyer [15]. This type of absorbing boundaries, as described for the 3-D case in Hatzigeorgiou and Beskos [10], is used in this work.

The artificial vertical boundaries in this work are discretized by rectangular vertical elements, which are actually the vertical faces of the 3-D solid elements (bricks) used to descretize the domain. The dimensions of those elements/faces are a*b as shown in Fig.3. To every nodal point one assigns two vertical and one horizontal (perpendicular to the vertical element/face) dashpots with values

$$c_s = (ab)\rho V_s, \quad c_n = (ab)\rho V_p \tag{1}$$

as shown in Fig.3, where ρ is the mass density and V_s and V_p are the shear wave and dilatational wave velocities, respectively, defined by

$$V_s = \sqrt{\frac{\quad}{\quad}}, \qquad V_p = \sqrt{\frac{\quad}{\quad}} \tag{2}$$

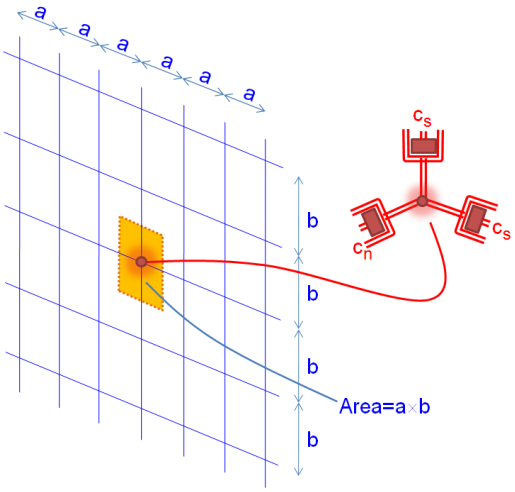

Figure 3: Vertical artificial boundary (external face of brick finite elements) and viscous dashpots

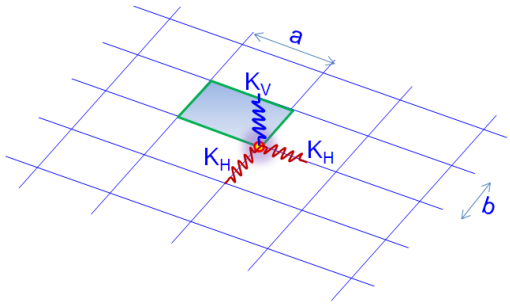

Figure 4: Bottom artificial boundary with nodal soil springs

Viscous dashpots are assigned to all the nodal points of the bottom face of the pavement domain in a similar way. At this bottom face one has also to introduce elastic springs at every node to simulate the supporting soil medium. The two horizontal spring constants K_H and the vertical spring constant K_V at every bottom node, as shown in Fig.4, are provided by the Mulliken and Karabalis [11] expressions

$$K_H = \text{————}, \quad K_V = \text{———} \tag{3}$$

where D is the half-length of the side of an equivalent square to the rectangular a*b of Fig.4, which is given by

$$D = \overline{\quad}/2 \tag{4}$$

The aforementioned dashpots and springs are appropriately introduced into the main ANSYS [9] program. For comparison purposes, in this work, rollers are also used at the three vertical faces and the bottom one.

3 MODELING OF MOVING VEHICLE LOADS

Consider a typical heavy vehicle (DAF truck model FAD CF75) of Fig.5 with four axles of concentrated loads $P_A = P_B = P_C = 16$ kN and $P_D = 32$ kN and axle distances $L_{AB} = 1.40$ m, $L_{BC} = 2.95$ m and $L_{CD} = 2.05$ m. Thus, the total axle length L = 6.40 m and the total weight of the vehicle is 80 kN = 18 kips, the standard weight used in US codes [1].

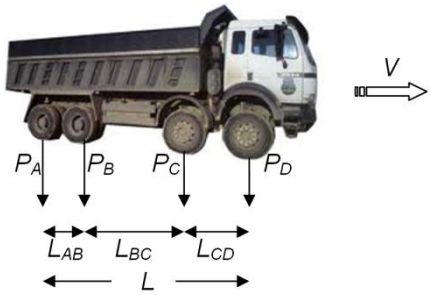

Figure 5: Typical heavy vehicle (truck) with four axles and total weight of 80 kN

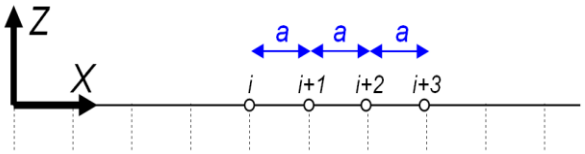

Figure 6: Top of discretized plane y=0 of the pavement system of Fig.1 with four successive nodes along the x axis

Consider next the top of the discretized plane y=0 of the pavement system of Fig.1 with four successive surface nodes along the direction of the vehicle's motion as shown in Fig.6. It is assumed that the distance a between two successive nodes is less than or equal to 1.0m so that $a<L_{AB}$. It is assumed that at time t=0 wheel D is on node i. At that instant one has $P_i=P_D$, $P_{i+1}=P_{i+2}=P_{i+3}=0$. For the vehicle to move a distance a the required time is $t_a=a/V$, where V is the constant speed of the vehicle. Hence wheel D will be on nodes i+1,i+2 and i+3 at times t_a, $2t_a$ and $3t_a$, respectively. In that case one has

$$P_{i+1}=P_D \text{ at } t=t_a, \quad P_{i+2}=P_D \text{ at } t=2t_a, \quad P_{i+3}=P_D \text{ at } t=3t_a \tag{5}$$

Without loss of generality, the subsequent analysis concentrates on node i+1. At time t=0 node i+1 is unloaded. After that, node i+1 starts being loaded since load P_D leaves node i and moves towards node i+1. Using isoparametric finite element concepts, load P_D is distributed to nodes i and i+1 in a linear manner during the time interval $0\le t\le t_a$ and the same happens for nodes i+1 and i+2 for the time interval $t_a\le t\le 2t_a$, as shown in Fig.7. The full unloading of node i+1 occurs after load P_D has reached node i+2. Taking into account that the vehicle considered has four axles, the total loading will be the result of the superposition of loads P_A, P_B, P_C and P_D, as shown in Fig.8. The loading configuration of Fig.8 for node i+1 is repeated for every other node of the pavement surface with the only difference being from node to node the commencement time of the above quadruple loading. Following this idea, one can model the 3-D distributed moving load as a sequence of many point loads along the x and y direction moving with a constant speed along the x direction.

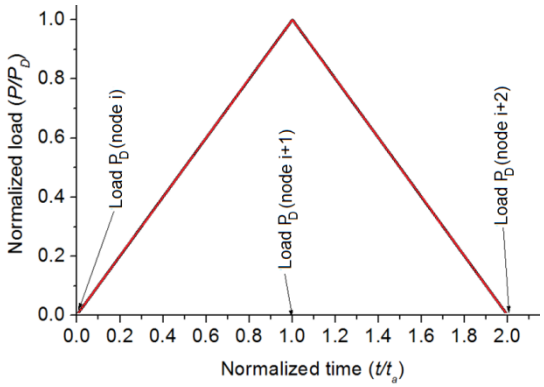

Figure 7: Loading of node *i*+1 by load P_D

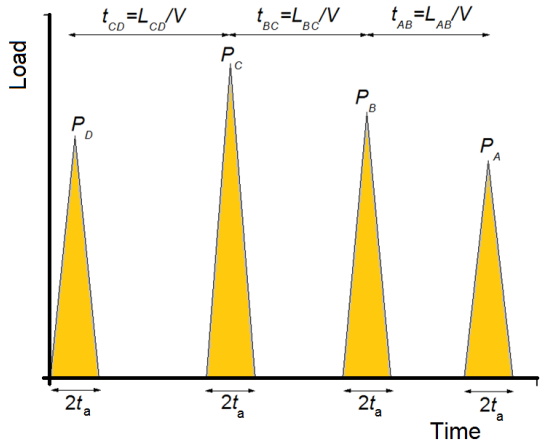

Figure 8: Total loading of node *i*+1 by the whole vehicle

The aforementioned procedure of load application in the time domain has been programmed and that program has been appropriately interfaced with the main ANSYS [9] program.

4 FINITE ELEMENT SOLUTION IN THE TIME DOMAIN

On the basis of the spatial modeling of the pavement structure of section 2, ANSYS [9] forms the mass matrix **M** and stiffness matrix **K** as well as the matrix equation of motion of that structure, which reads as

$$M\ddot{u} + Ku = F \tag{6}$$

where **u** is the vector of nodal displacements and **F** is the vector of nodal external forces on the surface z=0 coming from the moving wheel loads of the vehicle. The moving load starts at point A under zero initial conditions and terminates at point B, as shown in Fig.1. Structural damping is assumed to be zero.

Equation (6) is solved in the time domain to accommodate the in time evolution of the moving vehicle loads. The step-by-step time integration algorithm of Newmark [16] of the constant average acceleration type under zero initial conditions is employed in this work. This algorithm is unconditionally stable and provides highly accurate results provided an appropriate time step Δt has been selected.

The selection of an appropriate Δt is done on the basis of the guidelines in [16]. Thus if L_{el} is the maximum finite element length and V_p the dilatational wave velocity one has

$$\Delta t \leq L_{el}/V_p \tag{7}$$

An empirical relation provides Δt directly as [16]

$$\Delta t \leq 1/20f \tag{8}$$

where f is the highest loading frequency in Hz. Thus, on the assumption that for a truck the highest loading frequency f = 20 Hz, one obtains from (8) that $\Delta t \leq 0.0025$ sec. On the other hand, for L_{el}=0.15m (along the x axis) and V_p=500m/s, one has from (7) that $\Delta t \leq 0.3*10^{-3}$ sec. Thus, computations can commence with $\Delta t=0.6*10^{-3}$secs and contin-

ue with smaller values of Δt until convergence of the response results is established or an acceptable error is reached at convergence in case the exact value of the response is available.

5 NUMERICAL RESPONSE STUDIES

In this section validation studies of the proposed modeling are first presented. These have to do with comparisons on the basis of a uniform half-space under moving loads between numerical and analytical solutions. Comparisons on the basis of a layered half-space between numerical solutions for the cases of moving and stationary loads are also made. Numerically obtained responses for a single and a series of loads moving on a half-space medium are also compared.

5.1 Uniform half-space elastic medium under moving loads

Consider the road pavement structure of Fig.1 with identical properties in all three layers and the supporting soil, i.e., with $E = 50*10^6$ N/m^2, $v = 0.25$ and $\rho = 2000$ kg/m^3. The resulting domain becomes an elastic half-space with wave velocities of propagation $V_p = 173.2$ m/s and $V_s = 100$ m/s as obtained with the aid of Eqs (2). For this elastic half-space adopted from Eason [12], the Rayleigh wave velocity $V_R = 92$ m/s is the resonance wave velocity for a moving concentrated load. In road pavements, realistic velocities of moving vehicles do not exceed V = 50 m/s (180 km/h) and hence one deals with the subsonic case ($V<V_s$) and does not worry about resonance.

Table 1 lists the maximum values of the vertical displacement u_z at a depth of z = -1.0 m below the point Q (15, 0, 0) in the middle of the total length OC of the road (Fig.1) as obtained by ANSYS [9] for the velocity V=20m/s of the single concentrated moving load P = 80 kN, three types of boundary conditions and three time steps Δt together with the corresponding analytical values from Eason [12]. The case of the single concentrated load P is realized by assigning the values of $P_D = P = 16+16+16+32 = 80$ kN and $P_A = P_B = P_C = 0$ in the general four wheel vehicle case of Fig.5. Table 1 also shows the relative per cent error of the present numerical approximation as compared to the 'exact' analytic values of Eason [12]. It is observed that convergence of the numerical results is obtained for $\Delta t = 0.3*10^{-3}$sec for all cases of boundary conditions. However, only the error of the case of absorbing boundaries (about 2-3%) is considered acceptable for displacements, because naturally one expects the error to be higher for stresses and strains but no more than 10%, which is usually the limit for design purposes.

	Δt (secs)	Rollers at bottom	Rollers everywhere	Absorbing boundaries
Eason [12] u_z= $0.81608*10^{-3}$m	$0.6*10^{-3}$	u_z= $0.85186*10^{-3}$m e=4.38%	u_z= $0.826032*10^{-3}$m e=1.22%	u_z= $0.816635*10^{-3}$m e=0.08%
	$0.3*10^{-3}$	u_z= $0.878057*10^{-3}$m e=7.59%	u_z= $0.85980*10^{-3}$m e=5.36%	u_z= $0.836078*10^{-3}$m e=2.45%
	$0.15*10^{-3}$	u_z= $0.879081*10^{-3}$m e=7.72%	u_z= $0.857455*10^{-3}$m e=5.07%	u_z= $0.843428*10^{-3}$m e=3.35%

Table 1: Maximum vertical displacement u_z at depth z=-1.0m below Q due to a vertical point load P=80kN moving with a speed V=20m/s on the surface of half-space for three types of boundary conditions and three values of Δt.

Consider now the case of a moving distributed load on the surface of the half-space. The area in the full domain on which the load P=80 kN acts, on the basis of the adopted discretization as well as Huang [1], is A=0.45*0.30 m^2 yielding a pressure p=0.5926 MPa. Table 2 provides the maximum values of the vertical displacement u_z at a depth z=-1.0 m below Q due to the above pressure p moving at a speed V=20 m/s on the surface of the half-space for three types of boundary conditions and three values of Δt. Approximate analytical results from Eason [12] are also given in Table 2. It is seen from that table that convergence of the numerical results with acceptable error (about 2%) is obtained for $\Delta t=0.3*10^{-3}$secs for either the 'rollers everywhere' or the absorbing boundaries. It is also observed from Table 2 that the response to the distributed load is less than that to the point load, as expected.

Another comparison study on the basis of the elastic half-space model involved the maximum values of the displacement u_z as computed by using a single total load P = 80 kN and a series of four concentrated loads $P_A = P_B = P_C = 16$ kN and $P_D = 32$ kN, as shown in Fig.5. It was found that for the case of V = 20 m/s and Δt = 0.0003 secs, the maximum displacement u_z, as obtained for the case of the series of moving loads, is $0.352775*10^{-3}$ m, i.e., smaller than the corresponding one $0.836078*10^{-3}$ m for the case of the single moving load, as expected.

	Δt (secs)	Rollers at bottom	Rollers everywhere	Absorbing boundaries
Modified Eason[12] u_z= $0.800765*10^{-3}$m	$0.6*10^{-3}$	u_z= $0.785836*10^{-3}$m e=-1.86%	u_z= $0.752302*10^{-3}$m e=-6.05%	u_z= $0.748779*10^{-3}$m e=-6.49%
	$0.3*10^{-3}$	u_z= $0.819808*10^{-3}$m e=1.90%	u_z= $0.785013*10^{-3}$m e=-1.96%	u_z= $0.780815*10^{-3}$m e=-2.49%
	$0.15*10^{-3}$	u_z= $0.820634*10^{-3}$m e=2.48%	u_z= $0.786049*10^{-3}$m e=-1.84%	u_z= $0.782750*10^{-3}$m e=-2.25%

Table 2: Maximum vertical displacement u_z at depth z=-1.0 m below Q due to a vertical distributed load p=0.5926 MPa moving at speed V=20 m/s on surface of half-space for three types of boundary conditions and three values of Δt.

Since in pavement design, static analytic solutions for the uniform or the layered half space under distributed load are widely used [1], a comparison between analytical due to Boussinesq [13] and numerical results obtained here for the half-space under static distributed load is shown in Table 3. It is observed in that table that the error for the displacement is almost the same with that of the dynamic case (Table 2), while the error for stresses is higher, as expected. Furthermore, it is observed that for the numerical results $\sigma_x \neq \sigma_y$, as expected because of lack of axisymmetry in the numerical model.

	Analytic	Numerical	error%
u_z	$-0.781237*10^{-3}$m	$-0.762646*10^{-3}$m	-2.38
σ_z	$-36.2610*10^{-3}$MPa	$-34.9024*10^{-3}$MPa	-3.75
σ_x	$2.70265*10^{-3}$MPa	$2.60308*10^{-3}$MPa	-3.68
σ_y	$2.70265*10^{-3}$MPa	$2.79802*10^{-3}$MPa	-3.53

Table 3: Vertical deflection and stresses at z=-1.00 m below Q due to a vertical distributed static load p=0.5926 MPa acting on the surface of the uniform half-space.

5.2 Layered half-space elastic medium under moving loads

Consider the layered half-space model of Fig.1 with elastic material properties as described in section 2 under the moving with speed V=20 m/s distributed load p=0.5926 MPa. Using absorbing boundary conditions and $\Delta t=0.3*10^{-3}$ secs, Table 4 provides maximum vertical displacements, stresses and strains for the above pavement structure at z=-0.15m and -0.45m, usually needed for design purposes. The vertical deflection u_z at the surface of the top layer was found to be $-0.89667*10^{-3}$ m.

z(m)	u_z(m)	σ_z (MPa)	σ_x (MPa)	σ_y (MPa)	ε_z ($*10^{-3}$)	ε_x ($*10^{-3}$)	ε_y ($*10^{-3}$)
-0.15	$-0.849042*10^{-3}$	-0.692631	-0.244614	-0.207232	-0.551984	0.109700	0.211367
-0.45	$-0.668003*10^{-3}$	-0.111987	0.106403	0.108179	-0.465643	0.268868	0.278996

Table 4: Maximum vertical displacements, stresses and strains in elastic layered pavement structure under a moving distributed load with V=20 m/s.

Consider now the previous pavement structure under the same load, which is applied statically. Table 5 provides values for the same response quantities as Table 4 but for the static case. Values in parentheses indicate approximate analytical values obtained by the method of Odemark [14]. The static vertical deflection u_z at the surface of the pavement was found to be $-0.85730*10^{-3}$m numerically and $-0.91830*10^{-3}$m analytically. It is observed from Table 5 that while the numerical results for displacements are rather close to the approximate analytical ones, this is not always the case for stresses and strains. Finally, a comparison between the dynamic results of Table 4 and the static ones of Table 5 reveals that the former are always larger than the latter ones for displacements and in almost all the cases for stresses and strains.

z(m)	u_z(m)	σ_z (MPa)	σ_x (MPa)	σ_y (MPa)	ε_z ($*10^{-3}$)	ε_x ($*10^{-3}$)	ε_y ($*10^{-3}$)
-0.15	-0.813351 $*10^{-3}$ (-0.86250 $*10^{-3}$)	-0.4464 (-0.3890)	-0.09653 (-0.04512)	-0.06617 (-0.04512)	-0.4895 (-0.88217)	-0.0592 (0.26272)	0.1180 (0.26272)
-0.45	-0.632773 $*10^{-3}$ (-0.69230 $*10^{-3}$)	-0.08217 (-0.0742)	0.05167 (0.00092)	0.05439 (0.00092)	-0.46299 (0.93669)	0.26063 (-0.37789)	0.276045 (-0.37789)

Table 5: Displacements, stresses and strains in elastic layered pavement structure under static distributed load (approximate analytic values are in parentheses).

6 CONCLUSIONS

- An effort has been made to construct in the framework of the ANSYS computer program a general 3-D model for the simulation in the time domain of the dynamic response of a flexible road pavement to the motion of a vehicle under linear elastic material behavior.

- This modeling required the construction of a special moving loads program, which makes possible the loading of the road pavement structure as the vehicle moves at a constant speed and is connected with the main ANSYS program as well as special viscous absorbing boundaries at the vertical faces and bottom face of the domain to avoid wave reflections at its boundaries and special springs at its bottom face to simulate the supporting soil.

- The above model was used to study the dynamic and static responses of the pavement to moving or stationary loads for the cases of the homogeneous half-space and the layered half-space and compare them against those from analytical methods.

- Comparison and convergence studies led to the optimum domain model and its discretization and an approximate time step for obtaining solutions of acceptable accuracy at a reasonable computational cost.

- It was found that dynamic response is always higher than the corresponding static one and that increasing values of vehicle speed increase the pavement response. Furthermore, it was also found that a series of moving loads or a distributed moving load result in a lower response than a single moving load of intensity equal to the sum of intensities of the series of loads or to the resultant force of the distributed load.

- More work is required in order to complete this study that includes the effect of viscous damping on the response and consideration of linear viscoelastic material behavior for the top (asphalt) layer as well as comparisons with experimental results.

ACKNOWLEDGEMENT

The first author (Niki D.Beskou) acknowledges with thanks the support provided to her by the 'IKY fellowships of excellence for postgraduate studies in Greece-Siemens program'.

REFERENCES

[1] Y.H. Huang, *Pavement analysis and design*, Pearson Prentice-Hall, Upper Saddle River, N.Jersey, U.S.A., 2004.

[2] N.D. Beskou and D.D. Theodorakopoulos, Dynamic effects of moving loads on road pavements: A review, *Soil Dynamics and Earthquake Engineering*, **31**, 547-567, 2011.

[3] Y.H. Cho, B.F. McCulough, J. Weissmann, Considarations on finite element method application in pavement structural analysis, *Transportation Research Record*, **1539**, 96-101, 1996.

[4] H. Grundmann, M. Lieb, E. Trommer, The response of a layered half-space to traffic loads moving along its surface, *Archive of Applied Mechanics*, **69**, 55-67, 1999.

[5] S.H. Ju, Finite element investigation of traffic induced vibrations, *Journal of Sound and Vibration*, **321**, 837-853, 2009.

[6] S. Hirose, Boundary element modeling and analysis of moving loads in time and frequency domain, N.Chouw, G.Schmid eds., *Wave 2000*, A.A.Balkema, Rotterdam, 2000, 71-82.

[7] Y.B. Yang, H.H. Hung, A 2.5D finite/infinite element approach for modeling visco-elastic bodies subjected to moving loads, *International Journal for Numerical Methods in Engineering*, **51**, 1317-1336, 2001.

[8] J.H. Lee, J.K. Kim, J.L. Tassoulas, Dynamic analysis of a layered half-space subjected to moving line loads, *Soil Dynamics and Earthquake Engineering*, **47**, 16-31, 2013.

[9] ANSYS, ANSYS LS-DYNA User's Guide, Release 13, ANSYS Inc. Southpointe, Canonsburg, PA, USA, 2010.

[10] G.D. Hatzigeorgiou, D.E. Beskos, Soil-structure interaction effects on seismic inelastic analysis of 3-D tunnels, *Soil Dynamics and Earthquake Engineering*, **30**, 851-861, 2010.

[11] J.S. Mulliken, D.L. Karabalis, Discrete model for dynamic through-the-soil coupling of 3-D foundations and structures, *Earthquake Engineering and Structural Dynamics*, **27**, 687-710, 1998.

[12] G. Eason, The stresses produced in a semi-infinite solid by a moving surface force, *International Journal of Engineering Science*, **2**, 581-609, 1965.

[13] J.V. Boussinesq, *Applications des Potentiels a L'Etude de l'Equilibre et du Movement des Solides Elastiques*, Gauthier Villars, Paris, 1885.

[14] N. Odemark, *Investigations as to the elastic properties of soils and design of pavements according to the theory of elasticity,* Meddelanden 77 fran Statens Vaginstitut, Stockholm, Sweden, 1949.

[15] J. Lysmer, R.L. Kuhlemeyer, Finite dynamic model for infinite media, *Journal of the Engineering Mechanics Division of ASCE,* **95(4)**, 859-877, 1969.

[16] K.J. Bathe, *Finite element procedures*, Prentice Hall, Englewood Cliffs, New Jersey, USA, 1996.